

# Programmable Valves: a Solution to Bypass Deadband Problem of Electro-Hydraulic Systems

Song Liu and Bin Yao

**Abstract**—The closed-center PDC/servo valves have overlapped spools to prevent internal leakage so that the system can hold a position even when the power is off. However, the over-lapped spools also introduce deadbands, which are sandwiched by plant dynamics and valve dynamics. The sandwiched deadbands would degrade the achievable control performance and are very difficult to deal with. Instead of trying to solve this sandwiched deadband control problem via complicated advanced controls with limited improvement of achievable performance, this paper bypasses this problem with the use of both valve hardware redesign and advanced controls to overcome this deadband problem completely. Specifically, the hardware is based on the programmable valves, a unique combination of five independently controlled poppet type cartridge valves. This paper will compare the programmable valves with traditional PDC/servo valves and demonstrate the ability of completely solving the deadband control problem of the electro-hydraulic systems using the programmable valves. A nonlinear model based Adaptive Robust Controller with deadband compensation is designed for PDC/servo valve and a two-level coordinate controller is designed for programmable valves to maximize the achievable control performance of each. Experimental results show that the best tracking performance is achieved through the programmable valves.

## I. INTRODUCTION

Closed-center valves (either servo valve or proportional directional control (PDC) valves) are widely used in industry for motion or velocity control. An over-lapped spool is intentionally added in this kind of valves to prevent internal leakage so that the system can hold a position even when the power is off. A side effect of the over-lapped spool is the deadband problem, which in turn degrades the achievable control performance or even destabilizes the closed-loop system if not properly dealt with.

A conventional method to solve this problem is to add an inverse deadband function into the system to cancel or compensate the deadband effect [1], [2]. This method requires two conditions: a) the deadband property is known or accurately estimated and b) the valve dynamics is fast enough to be neglected. The first condition can be achieved through off-line system identification [2] or through on-line parameter adaptation [3]. The second condition usually does not hold unless sacrificing some system performance, i.e., to limit the closed-loop system bandwidth so that the valve dynamics (usually pretty slow for PDC valves, less than 10Hz) is "fast enough" compared with the closed-loop bandwidth.

Another way to solve this problem is to consider the deadband being sandwiched by valve dynamics and actuator dynamics. The general sandwiched deadband control

problem is solved by Tao in [3], [4], [5]. But to apply Tao's method to electro-hydraulic systems, the feedback of valve-spool position is required. Although the spool position feedback is available in some PDC valves, it is not a general valve configuration and would definitely increase the system cost. In addition, the spool position measurement is normally too noisy to help increasing the bandwidth significantly [2].

In this paper, the sandwiched deadband problem is bypassed by a new valve configuration—the programmable valves, a unique combination of five independently controlled poppet type cartridge valves. The programmable valves, while having the ability to hold position due to the virtually zero internal leakages when the cartridge valves are shut off, are able to bypass the sandwiched deadband problem completely when controlled properly. The five independently controlled cartridge valves increased the flexibility and controllability and enable not only better tracking performance but also secondary control purposes, such as energy saving. Our previous works have already shown the significant energy saving obtained through the programmable valves [6], [7]. This paper will compare the programmable valves with traditional PDC/servo valves and demonstrate the ability of completely solving the deadband control problem of the electro-hydraulic systems using the programmable valves.

This paper is organized as follows. The programmable valves configuration is introduced first in section II. Section III analyzes the deadband of closed-center PDC/servo valves and poppet valves and reveals the difference of the deadbands. A nonlinear model based Adaptive Robust Controller with deadband compensation (section IV) is designed for PDC/servo valve and a two-level coordinate controller (section V) is designed for programmable valves to maximize the achievable control performance of each. Comparative experimental results are provided before the conclusions.

## II. PROGRAMMABLE VALVES CONFIGURATION

The programmable valves are composed of five independently controlled poppet type cartridge valves, as shown in Fig. 1. Not only can this configuration fulfil all four-way PDC/servo valve's functionalities, but also enables accurate control and the use of regeneration flow through the cross port valve (valve #3).

When the programmable valves in Fig. 1 are used, the meter-in and meter-out flow  $Q_1$  and  $Q_2$  are given by,

$$\begin{aligned} Q_1 &= Q_{v2} - Q_{v1} - Q_{v3} \\ Q_2 &= -Q_{v3} - Q_{v4} + Q_{v5} \end{aligned} \quad (1)$$

where  $Q_{vi}$ , ( $i = 1, 2, \dots, 5$ ) are the flow through the  $i$ th cartridge valve. Therefore, when valve #2 and #5 are open

S. Liu is a Ph.D Research Assistant at the School of Mechanical Engineering, Purdue University, W. Lafayette, IN 47907, USA [liul@ecn.purdue.edu](mailto:liul@ecn.purdue.edu)

B. Yao is an Associate Professor at the School of Mechanical Engineering, Purdue University, W. Lafayette, IN 47907, USA [byao@ecn.purdue.edu](mailto:byao@ecn.purdue.edu)

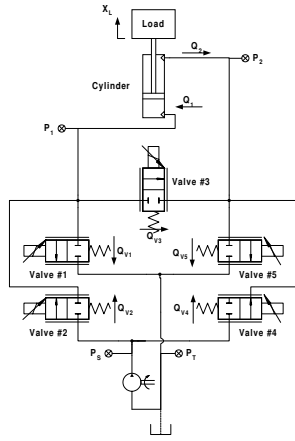


Fig. 1. Programmable Valves Configuration.

while other three are all closed, this configuration works similarly as PDC/servo valves to provide positive meter-in and meter-out flow; when valve #1 and #4 are open while other three are all closed, this configuration provides negative meter-in and meter-out flow like PDC/servo valves. When valve #3 is open, this configuration is capable to provide cross port regeneration flow provided that the necessary pressure conditions in the two cylinder chambers are met.

Another important advantage of the programmable valves is the independent control of the five cartridge valves. With the conventional PDC/servo valve, the meter-in and meter-out flow are coupled and can not be controlled independently due to the single input signal to the valve, therefore the pressures at the two cylinder chambers can not be controlled independently. On the other hand, with the programmable valves, all the flows,  $Q_{v1}$  through  $Q_{v5}$ , are controlled independently, therefore, meter-in and meter-out flows are decoupled and the pressures at the two cylinder chambers can be controlled independently. The increased controllability would result in better performance and enable secondary control objective such as energy saving [6].

### III. DEADBANDS OF CLOSED-CENTER VALVES VS. POPPET VALVES

The deadband of closed-center PDC/servo valve is due to the over-lapped spool, as shown in Fig. 2. It is obvious that the deadband is sandwiched by two dynamic blocks — valve dynamics and plant dynamics, as shown in Fig. 3. A common solution is to add a deadband inverse function (DBI) to cancel the deadband (DB). However, because the spool can not travel infinitely fast, the cancellation would never be perfect. This solution is economical, easy to implement and acceptable if one does not require too much for the tracking performance. On the other hand, when both performance (fast response and accurate tracking) and the ability of holding position when the valve is shut off are

desired, the above solution usually results in either limit cycle or large steady state error, and must be replaced with better and more complicate control schemes.

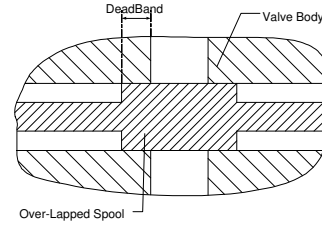


Fig. 2. Over-Lapped Spool of Closed-Center Valves.

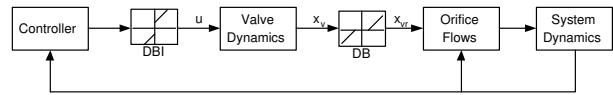


Fig. 3. PDC/servo Valve Controlled Hydraulic System.

The poppet type cartridge valves, as shown in Fig. 4, also have deadband, which is due to the fact that the input signal has to be large enough to overcome the spring force and static friction. Once the poppet moves, the orifice opens. Therefore, the deadband is the input deadband which is easy to cancel, as shown in Fig 5. In addition to this, the dynamic responses of the cartridge valves are usually much more faster than PDC valves. Neglecting cartridge valve dynamics is more reasonable than neglecting PDC valve dynamics.

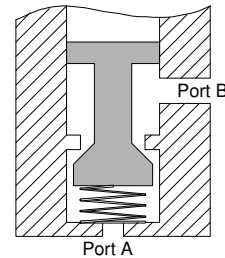


Fig. 4. Poppet Type Cartridge Valve.

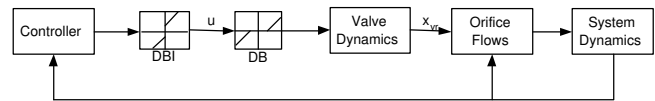


Fig. 5. Programmable Valves Controlled Hydraulic System.

### IV. MOTION CONTROL WITH PDC/SERVO VALVES

To test and compare the four-way PDC/servo valves and programmable valves, both valves are used to control the boom motion of an electro-hydraulic robot arm located at Ray. W. Herrick Laboratories. The Adaptive Robust Control technique, developed by Yao and Tomizuka [8], [9], would be applied to both systems to maximize the achievable performance of each. The controller design for the PDC/servo

valve controlled system with deadband compensation is described in this section, while the design for programmable valves controlled system will be introduced in the next section.

#### A. Dynamic Model

The boom motion dynamics of the electro-hydraulic robot arm with the other two joints (swing and stick) fixed can be described by [2], [6].

$$(J_c + m_L \ell_e^2) \ddot{q} = \frac{\partial x_L}{\partial q} (P_1 A_1 - P_2 A_2) - G_c(q) - m_L g \ell_g(q) - D_f \cdot \dot{q} + T(t, q, \dot{q}) \quad (2)$$

where  $q$  represents the boom joint angle,  $J_c$  is the moment of inertia of the boom without payload,  $m_L$  represents the mass of the unknown payload,  $G_c$  is the gravitational load of the boom without payload,  $x_L$  represents the boom hydraulic cylinder displacement,  $P_1$  and  $P_2$  are the head and rod end pressures of the cylinder respectively,  $A_1$  and  $A_2$  are the head and rod end areas of the cylinder respectively,  $D_f$  is the damping and viscous friction coefficient and  $T$  represents the lumped disturbance torque including external disturbances and terms like the unmodelled friction torque. The specific forms of  $J_c$ ,  $G_c$ ,  $\ell_g$ , and  $\ell_e$  are given in [2]. The

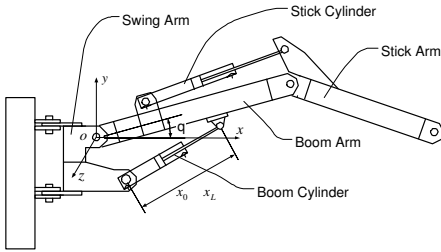


Fig. 6. Three Degree-of-Freedom Electro-Hydraulic Robot Arm.

inertial moment and the gravity force both depend on the unknown element  $m_L$ . As a result, the inertial moment and the gravity force are split into two components: the terms  $J_c$  and  $G_c(q)$  which contain only calculable quantities and the terms  $m_L g \ell_g(q)$  and  $m_L \ell_e^2$  which contain the unknown quantity  $m_L$ . The unknown terms have to be estimated later on-line via parameter adaptation.

Neglecting cylinder flow leakages, the hydraulic cylinder equations can be written as [10],

$$\begin{aligned} \frac{V_1(x_L)}{\beta_e} \dot{P}_1 &= -A_1 \dot{x}_L + Q_1 = -A_1 \frac{\partial x_L}{\partial q} \dot{q} + Q_{1M} + \tilde{Q}_1 \\ \frac{V_2(x_L)}{\beta_e} \dot{P}_2 &= A_2 \dot{x}_L - Q_2 = A_2 \frac{\partial x_L}{\partial q} \dot{q} - Q_{2M} + \tilde{Q}_2 \end{aligned} \quad (3)$$

where  $V_1(x_L) = V_{h1} + A_1 x_L$  and  $V_2(x_L) = V_{h2} - A_2 x_L$  are the total cylinder volumes of the head and rod ends including connecting hose volumes respectively,  $V_{h1}$  and  $V_{h2}$  are the initial control volumes when  $x_L = 0$ ,  $\beta_e$  is the effective bulk modulus.  $Q_1$  and  $Q_2$  are the supply and return flows respectively,  $Q_{1M}$  and  $Q_{2M}$  are supply and return flows satisfying the orifice equation.

$$\begin{aligned} Q_{1M} &= k_{q1} x_{vr} \sqrt{\Delta P_1} \\ Q_{2M} &= k_{q2} x_{vr} \sqrt{\Delta P_2} \end{aligned} \quad (4)$$

where  $k_{q1}$  and  $k_{q2}$  are orifice flow coefficients which can be obtained through off-line system identification,  $x_{vr}$  are the virtual valve spool displacement, and  $\Delta P_1$  and  $\Delta P_2$  are the pressure drops across the valve.

#### B. ARC Controller Design

Define a set of parameters as  $\theta = [\theta_1, \dots, \theta_6]^T$ ,  $\theta_1 = \frac{1}{J_c + m_L \ell_e^2}$ ,  $\theta_2 = \frac{D_f}{J_c + m_L \ell_e^2}$ ,  $\theta_3 = \frac{T_n}{J_c + m_L \ell_e^2}$ ,  $\theta_4 = \beta_e$ ,  $\theta_5 = \beta_e \tilde{Q}_{1n}$ ,  $\theta_6 = \beta_e \tilde{Q}_{2n}$ . It is practically to assume that all parameters and disturbances are bounded and the bounds can be estimated with *a priori* information.

Neglecting the valve dynamics, the system dynamics equations can be rewritten as:

$$\begin{aligned} \ddot{q} &= \frac{\theta_1}{J_c} \left[ \frac{\partial x_L}{\partial q} (P_1 A_1 - P_2 A_2) - G_c \right] + \frac{\theta_1}{\ell_e^2} g \ell_g \\ &\quad - \dot{q} \theta_2 + \theta_3 - \frac{1}{\ell_e^2} g \ell_g + \Delta \\ \dot{P}_1 &= -\frac{A_1}{V_1} \frac{\partial x_L}{\partial q} \dot{q} \theta_4 + \frac{\theta_4}{V_1} Q_{1M} + \frac{\theta_5}{V_1} + \Delta_{Q1} \\ \dot{P}_2 &= \frac{A_2}{V_2} \frac{\partial x_L}{\partial q} \dot{q} \theta_4 - \frac{\theta_4}{V_2} Q_{2M} - \frac{\theta_6}{V_2} + \Delta_{Q2} \end{aligned} \quad (5)$$

#### Step 1

Define a switching-function-like quantity as

$$z_2 = \dot{z}_1 + k_1 z_1 = \dot{q} - \dot{q}_r, \quad \dot{q}_r \triangleq \dot{q}_d - k_1 z_1 \quad (6)$$

where  $z_1 = q - q_d(t)$  is the output tracking error with  $q_d(t)$  being the reference trajectory. Differentiate (6) while noting (5)

$$\begin{aligned} \dot{z}_2 &= \theta_1 \left[ \frac{1}{J_c} \left( \frac{\partial x_L}{\partial q} P_L - G_c \right) + \frac{1}{\ell_e^2} g \ell_g \right] - \frac{1}{\ell_e^2} g \ell_g \\ &\quad - \dot{q}_r - \theta_2 \dot{q} + \theta_3 + \Delta \end{aligned} \quad (7)$$

where  $P_L = P_1 A_1 - P_2 A_2$  is defined as the load force. If we treat  $P_L$  as the control input to (7), we can synthesize a virtual control law  $P_{Ld}$  such that  $z_2$  is as small as possible. Since (7) has both parametric uncertainties  $\theta_1$  through  $\theta_3$  and uncertain nonlinearity  $\Delta$ , the ARC approach proposed by Yao [9] will be generalized to accomplish this system.

The design details are similar to those in [11], [2] and omitted. The resulting control function  $P_{Ld}$  consists of two parts given by

$$\begin{aligned} P_{Ld}(q, \dot{q}, \hat{\theta}_1, \hat{\theta}_2, \hat{\theta}_3, t) &= P_{Lda} + P_{Lds} \\ P_{Lda} &= \frac{\partial q}{\partial x_L} \left[ G_c + \frac{J_c}{\theta_1} \left( -\frac{\hat{\theta}_1}{\ell_e^2} g \ell_g + \hat{\theta}_2 \dot{q} - \theta_3 + \frac{1}{\ell_e^2} g \ell_g + \ddot{q}_r \right) \right] \\ P_{Lds} &= P_{Lds1} + P_{Lds2}, \quad P_{Lds1} = -\frac{J_c}{\theta_{1min}} \frac{\partial q}{\partial x_L} k_2 z_2 \end{aligned} \quad (8)$$

in which  $P_{Lda}$  functions as an adaptive model compensation, and  $P_{Lds}$  is a robust control law with  $k_2 > 0$ , and  $P_{Lds2}$  is chosen to satisfy the following robust performance conditions as in [11]

$$\begin{aligned} \text{i} \quad & z_2 \left\{ \frac{1}{J_c} \theta_1 \frac{\partial x_L}{\partial q} P_{Lds2} - \tilde{\theta}^T \phi_2 + \Delta \right\} \leq \varepsilon_2 \\ \text{ii} \quad & z_2 \frac{\partial x_L}{\partial q} P_{Lds2} \leq 0 \end{aligned} \quad (9)$$

where  $\varepsilon_2$  is a design parameter. If  $P_L$  were the actual control input, the adaptation function as defined in [2] would be

$$\begin{aligned} \tau_2 &= w_2 \phi_2 z_2, \\ \phi_2 &\triangleq \left[ \frac{1}{J_c} \left( \frac{\partial x_L}{\partial q_2} P_{Lda} - G_c \right) + \frac{1}{l_c^2} g l_g, -\dot{q}_2, 1, 0, 0, 0 \right]^T \end{aligned} \quad (10)$$

where  $w_2 > 0$  is a constant weighting factor.

### Step 2

Let  $z_3 = P_L - P_{Ld}$  denote the input discrepancy. Define  $Q_L = \frac{A_1}{V_1} Q_{1M} + \frac{A_2}{V_2} Q_{2M}$ . In this step, a virtual control flow  $Q_{Ld}$  will be synthesized so that  $z_3$  converges to zero or a small value with a guaranteed transient performance and accuracy.

From (5),

$$\begin{aligned} \dot{z}_3 &= \dot{P}_L - \dot{P}_{Ld} \\ &= \theta_4 \left[ Q_L - \left( \frac{A_1^2}{V_1} + \frac{A_2^2}{V_2} \right) \frac{\partial x_L}{\partial q} \dot{q} \right] + \frac{A_1}{V_1} \theta_5 + \frac{A_2}{V_2} \theta_6 \\ &\quad - \dot{P}_{Ldc} + A_1 \Delta_{Q1} - A_2 \Delta_{Q2} - \dot{P}_{Ldu} \end{aligned} \quad (11)$$

where

$$\begin{aligned} \dot{P}_{Ldc} &= \frac{\partial P_{Ld}}{\partial q} \dot{q} + \frac{\partial P_{Ld}}{\partial \hat{q}} \hat{q} + \frac{\partial P_{Ld}}{\partial t} \\ \dot{P}_{Ldu} &= \frac{\partial P_{Ld}}{\partial q} \left[ -\frac{\hat{\theta}_1}{J_c} \left( \frac{\partial x_L}{\partial q} P_L - G_c \right) - \frac{\hat{\theta}_1}{l_c^2} g l_g(q) \right. \\ &\quad \left. + \hat{\theta}_2 \dot{q} - \hat{\theta}_3 + \Delta \right] + \frac{\partial P_{Ld}}{\partial \hat{\theta}} \hat{\theta} \end{aligned} \quad (12)$$

in which  $\hat{q}$  represent the calculable part of  $\dot{q}$  given by

$$\hat{q} = \frac{\hat{\theta}_1}{J_c} \left[ \frac{\partial x_L}{\partial q} P_L - G_c \right] + \frac{\hat{\theta}_1}{l_c^2} g l_g - \hat{\theta}_2 \dot{q} + \hat{\theta}_3 - \frac{1}{l_c^2} g l_g \quad (13)$$

In (12),  $\dot{P}_{Ldc}$  is calculable and can be used in the construction of control functions, but  $\dot{P}_{Ldu}$  cannot due to various uncertainties. Therefore,  $\dot{P}_{Ldu}$  has to be dealt with via certain robust feedback in this step design.

In viewing (11),  $Q_L$  can be thought as the control input for (11) and step 2 is to synthesize a control function  $Q_{Ld}$  for  $Q_L$  such that  $P_L$  tracks the desired control function  $P_{Ld}$  synthesized in Step 1 with a guaranteed transient performance.

Similar to (8), the control function  $Q_{Ld}$  consists of two parts given by

$$\begin{aligned} Q_{Ld}(q, \dot{q}, P_1, P_2, \hat{\theta}, t) &= Q_{Lda} + Q_{Lds} \\ Q_{Lda} &= \left( \frac{A_1^2}{V_1} + \frac{A_2^2}{V_2} \right) \frac{\partial x}{\partial q} \dot{q} \\ &\quad - \frac{1}{\hat{\theta}_4} \left( \frac{A_1}{V_1} \hat{\theta}_5 + \frac{A_2}{V_2} \hat{\theta}_6 - \dot{P}_{Ldc} + \frac{\hat{\theta}_1}{J_c} \frac{\partial x}{\partial q} z_2 \right) \\ Q_{Lds} &= Q_{Lds1} + Q_{Lds2}, \quad Q_{Lds1} = -\frac{1}{\theta_{4min}} k_3 z_3 \end{aligned} \quad (14)$$

where  $k_3 > 0$ .

Like (9),  $Q_{Lds2}$  is a robust control function chosen to satisfy the following two robust performance conditions

$$\begin{aligned} z_3 \{ \theta_4 Q_{1Mds2} - \tilde{\theta}^T \phi_3 - \frac{\partial P_{Ld}}{\partial q_2} \Delta + A_1 \Delta_{Q1} - A_2 \Delta_{Q2} \} &\leq \varepsilon_3 \\ z_3 Q_{1Mds2} &\leq 0 \end{aligned} \quad (15)$$

where  $\varepsilon_3$  is a positive design parameter. The adaptation function as defined in [2] would be

$$\tau = \tau_2 + \phi_3 z_3 \quad (16)$$

where  $\phi_3$  is defined as:

$$\phi_3 \triangleq \begin{bmatrix} \frac{1}{J_c} \frac{\partial x_L}{\partial q} z_2 - \frac{\partial P_{Ld}}{\partial \hat{q}} \left[ \frac{1}{J_c} \left( \frac{\partial x_L}{\partial q} P_L - G_c \right) + \frac{1}{l_c^2} g l_g \right] \\ \frac{\partial P_{Ld}}{\partial \hat{q}} \dot{q} \\ - \frac{\partial P_{Ld}}{\partial \hat{q}} \\ Q_{Ld} - \left( \frac{A_1^2}{V_1} + \frac{A_2^2}{V_2} \right) \frac{\partial x_L}{\partial q} \dot{q} \\ \frac{A_1}{V_1} \\ \frac{A_2}{V_2} \end{bmatrix} \quad (17)$$

### Step 3

Once the control functions  $Q_{Ld}$  for  $Q_L$  is synthesized as given in (14), the control input with deadband compensation can be calculated by

$$u = DBI \left( \frac{Q_{Ld}}{\frac{A_1}{V_1} k_{q1} \sqrt{\Delta P_1} + \frac{A_2}{V_2} k_{q2} \sqrt{\Delta P_2}} \right) \quad (18)$$

where  $DBI(\cdot)$  represents inverse deadband function.

## V. MOTION CONTROL WITH THE PROGRAMMABLE VALVES

The difficulties in the control of five cartridge valves are dealt with through a coordinate two-level controller: the task level and the valve level controllers. Given the current working condition, the task level controller determines how to use the five cartridge valves to enable significant energy saving while without losing hydraulic circuit controllability for motion tracking, which is sometimes referred to as the working mode selection in hydraulic industry. The valve level controller uses an adaptive robust control technique to control the pressures in both chambers independently with selected working mode to obtain the dual objectives.

### A. Working Mode Selection

The task level controller determines how the five valves of the proposed programmable valves in Fig. 1 should be used in order to provide the required control flows for motion tracking while maintaining the lowest possible cylinder chamber pressures to reduce the flow losses for energy saving. Obviously, such a process is not unique due to the added flexibility of independently controlling each of these five valves. The working mode selection is task dependent. There are five tracking modes and three regulation modes. The tracking mode selection [6], shown in Table I, is based on the desired cylinder velocity  $\dot{x}_d$ , chamber pressures  $P_1$  and  $P_2$  and desired load pressure  $P_{lda}$  given in (8). The regulation mode selection is shown in Table II, where  $\varepsilon$  is a small preset tolerance.

### B. Off-side Pressure Regulation

The objective of the off-side pressure regulator is to keep the off-side pressure at a constant low pressure  $P_0$ . To illustrate the design procedure, this section designs a pressure regulator for those working modes, for which  $P_2$  is the off-side. The regulator design for  $P_1$  follows the same procedure and is omitted here.

The dynamics of  $P_2$  is described in (3) and (1). In order to use parameter adaptation to reduce parametric uncertainties to improve performance, it is necessary to linearly parameterize the system dynamics in terms of a set

TABLE I  
PROGRAMMABLE VALVES TRACKING MODE SELECTION

$\dot{x}_d$	$P_{lda}$	Valve Configuration	Off-side	Mode
$> 0$	$> 0$	$Q_1 = Q_{v2}$ $Q_2 = Q_{v5}$	$P_2$	T1
$> 0$	$< 0$	$Q_1 = Q_{v2} - Q_{v3}$ $Q_2 = -Q_{v3}$	$P_1$	T2
$< 0$	$> 0$ $P_1 > P_2$	$Q_1 = -Q_{v3}$ $Q_2 = Q_{v5} - Q_{v3}$	$P_2$	T3
$< 0$	$> 0$ $P_1 \leq P_2$	$Q_1 = -Q_{v1}$ $Q_2 = -Q_{v4}$	$P_2$	T4
$< 0$	$< 0$	$Q_1 = -Q_{v1}$ $Q_2 = -Q_{v4}$	$P_1$	T5

TABLE II  
PROGRAMMABLE VALVES REGULATION MODE SELECTION

$\dot{x}_d$	$x - x_d$	Valve Configuration	Off-side	Mode
$= 0$	$> \varepsilon$	$Q_1 = -Q_{v3}$ $Q_2 = Q_{v5} - Q_{v3}$	$P_2$	R1
$= 0$	$< -\varepsilon$	$Q_1 = Q_{v2}$ $Q_2 = Q_{v5}$	$P_2$	R2
$= 0$	<i>otherwise</i>	$Q_1 = 0$ $Q_2 = 0$		R3

of unknown parameters  $\theta_p$ .  $\theta_p$  is defined as  $\theta_p = [\theta_\beta, \theta_Q]^T$ , where  $\theta_\beta = \beta_e$  and  $\theta_Q = \beta_e \tilde{Q}_{2n}$ ,  $\tilde{Q}_{2n}$  is the nominal value of  $\tilde{Q}_2$ , i.e.  $\tilde{Q}_2 = \tilde{Q}_{2n} + \Delta_Q$ . The  $P_2$  dynamics can be rewritten as follows.

$$\dot{P}_2 = \frac{A_2}{V_2} \frac{\partial x_L}{\partial q_2} \dot{q}_2 \theta_\beta - \frac{\theta_\beta}{V_2} Q_{2M} - \frac{\theta_Q}{V_2} + \Delta_Q \quad (19)$$

The goal is to have the cylinder pressure regulated to a desired constant low pressure  $P_0$ . It is practical to assume that the parameters and  $\Delta_Q$  are bounded by some known bounds, because both bulk modulus  $\beta_e$  and the modelling error of the flow mapping are practically bounded and the bound can be found with *a priori* information.

Define the pressure regulation error as  $e_{p2} = P_2 - P_0$ , the error dynamics would be same as the pressure dynamics because  $P_0$  is constant.

$$\dot{e}_{p2} = -\frac{\theta_\beta}{V_2} Q_{2M} + \frac{A_2}{V_2} \frac{\partial x_L}{\partial q_2} \dot{q}_2 \theta_\beta - \frac{\theta_Q}{V_2} + \Delta_Q \quad (20)$$

$Q_{2M}$  is the control input and the control law can be defined as:

$$Q_{2M} = (k_{p2} + k_{p2s}) \frac{V_2}{\theta_{\beta min}} e_{p2} + A_2 \frac{\partial x_L}{\partial q_2} \dot{q}_2 - \frac{\hat{\theta}_Q}{\hat{\theta}_\beta} \quad (21)$$

where  $(A_2 \frac{\partial x_L}{\partial q_2} \dot{q}_2 - \frac{\hat{\theta}_Q}{\hat{\theta}_\beta})$  is the model compensation term and called as  $Q_{2Ma}$ ,  $k_{p2} > 0$ , and  $k_{p2s} \frac{V_2}{\theta_{\beta min}} e_{p2}$  is the robust term to dominate the parameter estimation error and unmodelled disturbances, which is chosen to satisfy the following conditions:

$$\begin{aligned} e_{p2} (k_{p2s} \frac{\theta_\beta}{\theta_{\beta min}} e_{p2} - \phi_{p2}^T \tilde{\theta}_{p2} + \Delta_Q) &\geq -\varepsilon_p \\ k_{p2s} &\geq 0 \end{aligned} \quad (22)$$

where  $\varepsilon_p$  is a positive design parameter.

The parameter adaptation law is defined as

$$\dot{\hat{\theta}}_p = Proj_{\theta_p} (\Gamma_{off} \cdot \phi_{p2} \cdot e_{p2}) \quad (23)$$

where  $\Gamma_{off}$  is positive definite diagonal adaptation rate matrix, and  $\phi_{p2} = [\frac{A_2}{V_2} \frac{\partial x_L}{\partial q_2} \dot{q}_2 - \frac{Q_{2Ma}}{V_2}, -\frac{1}{V_2}]^T$ .

The above adaptive robust control law (21) and adaptation law (23) provides prescribed transient response and final tracking accuracy in general and asymptotic tracking in the absence of uncertain disturbance. Theoretical proof of standard ARC performance can be found in [9], [8], [12].

### C. Working-side Motion Controller Design

In this section, an ARC controller is designed for those working modes, for which  $P_1$  is the working-side. The controller design for  $P_2$  follows the same procedure and is omitted here.

The parameter definition and the first design step are same as those in Section IV-B.

#### Step 2

Let  $z_3 = P_L - P_{Ld}$  denote the input discrepancy. In this step, a virtual control flow will be synthesized so that  $z_3$  converges to zero or a small value with a guaranteed transient performance and accuracy.

From (5),

$$\begin{aligned} \dot{z}_3 &= \dot{P}_L - \dot{P}_{Ld} \\ &= -\left(\frac{A_1^2}{V_1} + \frac{A_2^2}{V_2}\right) \frac{\partial x_L}{\partial q_2} (q)_2 \theta_4 + \frac{A_2}{V_2} \theta_4 Q_{2M} + \frac{A_1}{V_1} \theta_5 + \frac{A_2}{V_2} \theta_6 \\ &\quad - \dot{P}_{Ldc} + \frac{A_1}{V_1} \theta_4 Q_{1M} + A_1 \Delta_{Q1} - A_2 \Delta_{Q2} - \dot{P}_{Ldu} \end{aligned} \quad (24)$$

where  $\dot{P}_{Ldc}$  and  $\dot{P}_{Ldu}$  were defined in (12).

In viewing (24),  $Q_{1M}$  can be thought as the control input for (24) and step 2 is to synthesize a control function  $Q_{1Md}$  for  $Q_{1M}$  such that  $P_L$  tracks the desired control function  $P_{Ld}$  synthesized in Step 1 with a guaranteed transient performance.

Similar to (8), the control function  $Q_{1Md}$  consists of two parts given by

$$\begin{aligned} Q_{1Md}(q_2, \dot{q}_2, P_1, P_2, \hat{\theta}, t) &= Q_{1Mda} + Q_{1Mds} \\ Q_{1Mda} &= \frac{V_1}{A_1 \hat{\theta}_4} \left\{ -\frac{\hat{\theta}_1}{J_c} \frac{\partial x_L}{\partial q_2} z_2 + \hat{\theta}_4 \left[ \left( \frac{A_1^2}{V_1} + \frac{A_2^2}{V_2} \right) \frac{\partial x_L}{\partial q_2} \dot{q}_2 \right. \right. \\ &\quad \left. \left. - \frac{A_2}{V_2} Q_{2M} \right] - \hat{\theta}_5 \frac{A_1}{V_1} - \hat{\theta}_6 \frac{A_2}{V_2} + \dot{P}_{Ldc} \right\} \\ Q_{1Mds} &= Q_{1Mds1} + Q_{1Mds2}, \quad Q_{1Mds1} = -\frac{V_1}{A_1 \theta_{4min}} k_3 z_3 \end{aligned} \quad (25)$$

where  $k_3 > 0$ .

Like (9),  $Q_{1Mds2}$  is a robust control function chosen to satisfy the following two robust performance conditions

$$\begin{aligned} z_3 \{ \theta_4 Q_{1Mds2} - \tilde{\theta}^T \phi_3 - \frac{\partial P_{Ld}}{\partial q_2} \Delta + A_1 \Delta_{Q1} - A_2 \Delta_{Q2} \} &\leq \varepsilon_3 \\ z_3 Q_{1Mds2} &\leq 0 \end{aligned} \quad (26)$$

where  $\varepsilon_3$  is a positive design parameter. The adaptation function would be

$$\tau = \tau_2 + \phi_3 z_3 \quad (27)$$

where  $\phi_3$  is defined as:

$$\phi_3 \triangleq \begin{bmatrix} \frac{1}{J_c} \frac{\partial x_L}{\partial q_2} z_2 - \frac{\partial P_{Ld}}{\partial q_2} \left[ \frac{1}{J_c} \left( \frac{\partial x_L}{\partial q_2} P_L - G_c \right) + \frac{1}{I_c} g I_g \right] \\ \frac{\partial P_{Ld}}{\partial q_2} \dot{q}_2 \\ - \frac{\partial P_{Ld}}{\partial q_2} \\ - \left( \frac{A_1^2}{V_1} + \frac{A_2^2}{V_2} \right) \frac{\partial x_L}{\partial q_2} \dot{q}_2 + \frac{A_2}{V_2} Q_{2M} + \frac{A_1}{V_1} Q_{1Ma} \\ \frac{A_1}{V_1} \\ \frac{A_2}{V_2} \end{bmatrix} \quad (28)$$

### Step 3

Once the control functions  $Q_{1Md}$  for  $Q_{1M}$  is synthesized as given in (25), the next step is to use the pressure compensated inverse valve mappings to calculate the specific valve control voltage command to provide the desired "flows"— $Q_{1Md}$ . The nonlinear pressure compensated valve mapping can be obtained through off-line experiments and builds into a look-up table.

## VI. COMPARATIVE EXPERIMENTAL RESULTS

For comparison, a closed-center four-way PDC valve (*Vickers KBFDG4V-5-2C50N-Z-PE7-H7-10*), a critical center servo valve (*Parker BD760AAAN10*) and the programmable valves (the combination of five proportional poppet type cartridge valves — *Vickers EPV10-A-8H-12D-U-10*) are used to control the boom motion of electro-hydraulic arm located at Ray. W. Herrick Laboratories. Same adaptive robust controller and same gains are used for the three cases. The task is to control the arm to track a desired point-to-point motion trajectory shown in Fig. 7. The controller gains are chosen to be  $k_1 = k_2 = k_3 = 12$ , adaptation rate be  $\Gamma = \text{diag}\{1e-10, 1e-10, 2e-8, 8e4, 1e-4, 1e-4\}$ . Additional gain for the off-side regulator for programmable valves is  $k_{off} = 20$ , adaptation rates for off-side regulation are  $\Gamma_{off} = \text{diag}\{2e4, 1e-6\}$ .

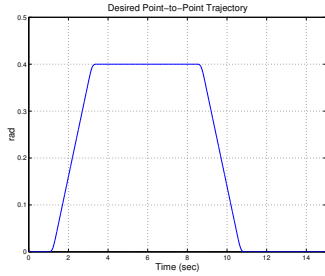


Fig. 7. Desired Point-to-Point Trajectory.

The experiments were done for PDC valve without/with deadband compensation, servo valve and programmable valves. The tracking errors are shown in Fig. 8. Not surprisingly, the PDC valve without deadband compensation exhibits the largest tracking error both at transient and steady state. The PDC valve's performance was greatly improved by the simple deadband compensation as shown in Fig. 8. Both servo valve and programmable valves show excellent tracking performances, but the programmable valves have shorter transient period and prescribed steady state tracking error.

## VII. CONCLUSIONS

The deadband control problem of electro-hydraulic systems is completely solved through hardware reconfiguration and advanced control technique. The sandwiched deadband of PDC/servo valves is bypassed through the use of the programmable valves, whose deadband is at the input side and much easier to compensate than the sandwiched deadband. The task-level controller smartly figures out the working modes according to the available information, and the valve-level controller utilizes advanced nonlinear

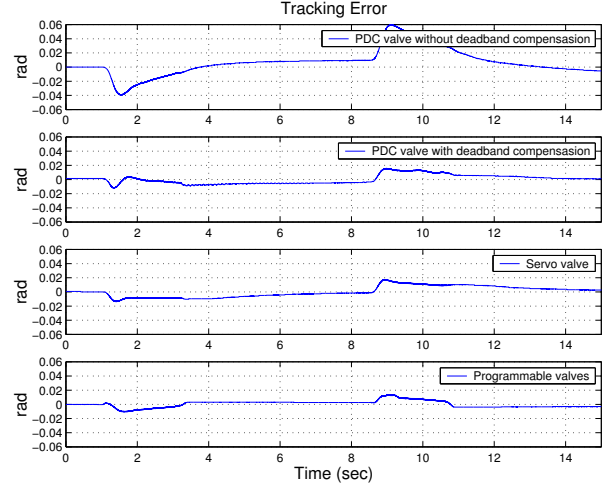


Fig. 8. Tracking Performance.

adaptive robust control technique to guarantee prescribed transient and steady state performance in the existence of model uncertainties and disturbances. The programmable valves, having virtually zero internal leakages, fast response speed, full functionality of PDC/servo valves and more flexibility and controllability, are promising alternatives of PDC/servo valves. Experimental results confirm that best tracking performance is obtained through the programmable valves.

## REFERENCES

- [1] J. D. Fortgang, L. E. George, and W. J. Book, "Practical implementation of a dead zone inverse on a hydraulic wrist," in *Proc. of IMECE2002*, vol. IMECE2002-39351, New Orleans, Louisiana, 2002.
- [2] F. Bu and B. Yao, "Nonlinear adaptive robust control of hydraulic actuators regulated by proportional directional control valves with deadband and nonlinear flow gain coefficients," in *Proc. of American Control Conference*, Chicago, 2000, pp. 4129–4133.
- [3] G. Tao and P. V. Kokotovic, *Adaptive Control of Systems with Actuator and Sensor Nonlinearities*. John Wiley & Sons, Inc, 1996.
- [4] A. Taware, G. Tao, and C. Teolis, "An adaptive dead-zone inverse controller for systems with sandwiched dead-zones," in *Proceedings of the American Control Conference*, Arlington, VA, 2001, pp. 2456–2461.
- [5] —, "Neural-hybrid control of systems with sandwiched dead-zones," in *Proceedings of the American Control Conference*, Arlington, VA, 2001, pp. 594–599.
- [6] S. Liu and B. Yao, "Energy-saving control of single-rod hydraulic cylinders with programmable valves and improved working mode selection," *SAE Transactions - Journal of Commercial Vehicle*, pp. 51–61, 2002, sAE 2002-01-1343.
- [7] —, "Coordinate control of energy-saving programmable valves," in *ASME International Mechanical Engineering Congree and Exposition*, Wahsington, D.C., 2003, iMECE 2003-42668.
- [8] B. Yao and M. Tomizuka, "Adaptive robust control of siso nonlinear systems in a semi-strict feedback form," *Automatica*, vol. 33, no. 5, pp. 893–900, 1997.
- [9] B. Yao, "High performance adaptive robust control of nonlinear systems: a general framework and new schemes," in *Proc. of IEEE Conference on Decision and Control*, 1997, pp. 2489–2494.
- [10] H. E. Merritt, *Hydraulic Control Systems*. John Wiley & Sons, 1967.
- [11] B. Yao, F. Bu, J. T. Reedy, and G. T. Chiu, "Adaptive robust control of single-rod hydraulic actuators: Theory and experiments," *The IEEE/ASME Trans. on Mechatronics*, vol. 5, no. 1, pp. 79–91, 2000.
- [12] B. Yao and M. Tomizuka, "Adaptive robust control of mimo nonlinear systems in a semi-strict feedback form," *Automatica*, vol. 37, no. 9, pp. 1305–1321, 2001.